RADARSAT-2 Polarimetric SAR Data for Urban Land Cover Classification: A Multitemporal Dual-Orbit Approach

Yifang Ban and Xin Niu
Geoinformatics, Royal Institute of Technology-KTH, Stockholm, Sweden; yifang@kth.se

Abstract: This research investigates multitemporal dual-orbit RADARSAT-2 polarimetric SAR data for urban land cover classification using an object-based support vector machine (SVM). Six-date RADARSAT-2 high-resolution SAR data in both ascending and descending orbits were acquired in the rural-urban fringe of the Greater Toronto Area during the summer of 2008. The major landuse/land-cover classes include high-density residential area, low-density residential area, industrial and commercial area, construction site, park, golf course, forest, pasture, water and two types of agricultural crops. The results show that multitemporal SAR data improve urban land cover classification and the best classification result is achieved using data from all six-dates. However, similar accuracies could be achieved using only three-date data from both ascending and descending orbits with relatively longer temporal span. Combinations of SAR data with relatively short temporal span are observed to yield lower classification accuracy. Similarly, combinations of SAR data from either ascending or descending orbit alone yield lower accuracy than the combinations of ascending and descending data. The results indicate that the combination of both the ascending and descending spaceborne SAR data with appropriate temporal span are suitable for urban land cover mapping.

Keywords: RADARSAT-2; Polarimetric SAR; Urban Land cover; Object-based; Support Vector Machines, Ascending and Descending Orbit

1. Introduction

To make rational policies for sustainable urban development, it is essential to collect up-to-date and reliable information on the current state of urban areas, such as urban land cover/land-use, through remote sensing. Among many remote sensing technologies, Synthetic Aperture Radar (SAR) has the capability to acquire data with unique information independent of cloud cover or solar illumination conditions. With the launch of advanced spaceborne SAR sensors such as RADARSAT-2 SAR and TerraSAR-X, multitemporal fully polarimetric SAR data in high-resolution become available. Several recent studies have demonstrated the usefulness of polarimetric SAR for urban land cover mapping [1]-[6]. However, urban mapping using such data still remains a challenge due to several factors. First, higher resolution data introduces higher variance which is more difficult to process using traditional pixel-based methods. Object-based methods [7], on the other hand, have been increasingly used in the urban mapping with reasonable successful [8][9], since more information such as the object features and spatial relationships could be explored in the analysis. Another challenge is how to effectively classify segments from multitemporal polarimetric SAR data. Considering the classification performance, several studies showed that Support Vector Machine is suitable for classification of multitemporal or multi-source data since there is no requirement of the statistic model for the data to be classified [10]-[12]. The superiority of SVM to other classifiers in the object-based analysis has been reported by various studies (e.g. [9], [13], [14]). However, most of those evaluations are conducted on the optical data or single-parameter SAR data. Very few studies investigated object-based SVM for classification of

multitemporal polarimetric SAR data. Therefore, the objective of this research is to investigate multitemporal RADARSAT-2 polarimetric SAR data for detailed urban land cover classification using an object-based SVM.

2. Study area and data description

The study area is situated in the northern urban-rural fringe of the Greater Toronto Area (GTA), Ontario, Canada. The GTA is the most populous metropolitan area in Canada and is one of the fastest growing urban areas in North America. The urban growth is encroaching on the Oak Ridges Moraine, an environmentally significant and sensitive area that lies north of Toronto [15]. The main land use/land-cover types are high-density residential areas (HD), low-density residential areas (LD), industrial and commercial areas (Ind.), construction areas (Cons.), parks, golf courses, forests, water, pasture and two types of crops.

Six-date RADARSAT-2 fine-beam Polarimetric SAR data were acquired over the study area during June to September in 2008. Those single look complex products include observations from HH, HV, VH and VV polarizations with nominal pixel spacing of 4.7 and 5.1 meters in the range and azimuth directions respectively. The centre frequency of this beam mode is 5.4GHz, i.e., C-band. The scenes covered by the ascending and descending observations in the GTA area are marked in Fig. 1.

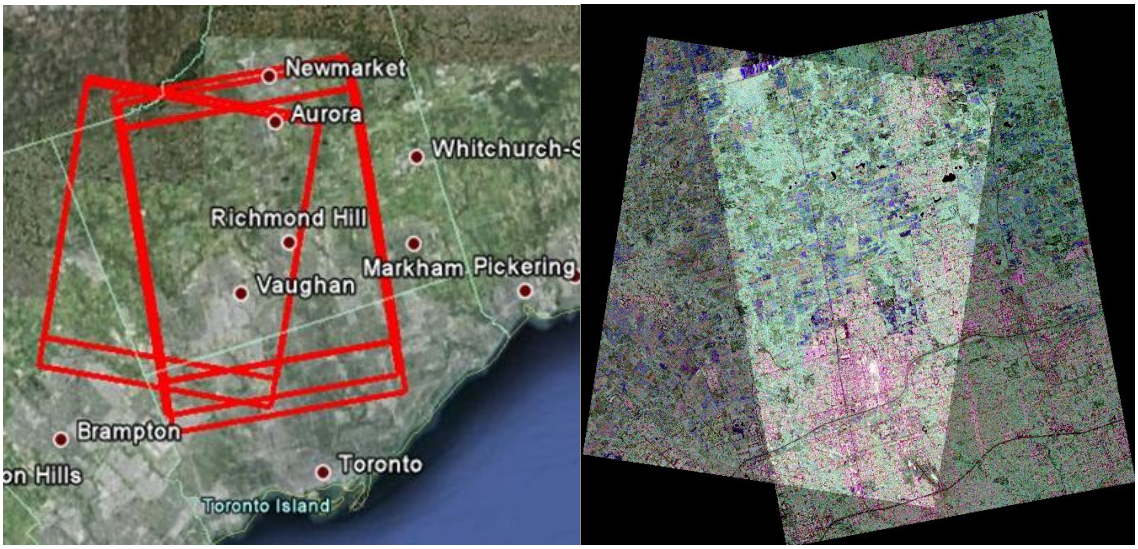

Figure 1. The Study Area: Rural-Urban Fringe of GTA, Ontario, Canada

The six-date data could be divided into two groups according to ascending or descending orbital mode. All data were collected in similar incident angles, thus the difference of using the two orbital mode images are mainly introduced by the radar look-directions. The data from according to ascending orbits are expected to complement each other by observing urban areas from two different look directions. The SAR data were acquired in the summer with peak vegetation season to improve the differentiation between built-up classes and vegetation classes. Detailed descriptions of these images are given in Table 1.

Table 1. RADARSAT-2 Fine-Beam Polarimtetric SAR Imagery

Data	Orbit Mode	Incident angle	Code number
June 11 2008	Ascending	40.18~ 41.59	A1
June 19 2008	Descending	40.22~ 41.62	D1
July 05 2008	Ascending	40.18~ 41.60	A2
August 06 2008	Descending	40.20~ 41.61	D2
August 22 2008	Ascending	40.17~ 41.59	A3
September 15 2008	Ascending	40.17~ 41.59	A4

3. Methodology

3.1. Geometric correction of SAR images

To remove the relief displacements introduced by the terrain and the opposite look-directions, each raw data was orthorectified using the RADARSAT-2 orbital parameters and a DEM with resolution of 30m. Then the multitemporal data are registered to the National Topographic Database (NTDB) vector database.

3.2. Selection of polarimetric SAR parameter sets

Based on our previous research [6],[9], the compressed Logarithmic Pauli parameter performed better than other polarimetric SAR parameters for object-based classification in urban areas. Therefore, compressed Logarithmic Pauli polarimetric parameter sets are selected for comparison of multitemporal classifications.

3.3. Segmentation

The segmentation is first performed on the compressed 8-bit Pauli images from all dates filtered by the refined Lee filter with window size of 7x7. Then this segmentation result is used to segment SAR data of various multitemporal and orbital combinations. The advantage of using the same segmentation is that same training objects can be used for all classifications. The potential issue is that the classification accuracies produced from multitemporal combinations of images from less dates could be higher since the segmentation of six-date SAR data is better than that of other datasets. In this study, segmentations are implemented in Definiens eCognition and the segment scale is set as 50.

3.4. Object-based SVM classification

Our previous research demonstrated that the object-based SVM classification of multitemporal SAR data in urban areas is superior than object-based NN classification [6]. Therefore the object-based SVM is adopted and implemented in LIBSVM [16]. There are many kernel functions used to map the input vectors into the high dimensional space. In our experiments, Radial Basis Function (RBF) is selected as the mapping kernel function:

$$k(x_i, x_j) = \exp(-\gamma \parallel x_i - x_j \parallel^2), \gamma > 0 \quad (1)$$

While using SVM to perform classifications with the RBF kernel, the optimization of two parameters is necessary to improve the predictive accuracy: The penalty value C and kernel parameter γ. In this study, the best parameters are selected from a limited searching grid through a cross-validation process. More information about SVM techniques is given in [17].

Using the SVM classifier, high-density residential areas, low-density residential areas, industrial and commercial areas, construction areas, forests, golf courses, parks, water, pasture and two types of crops are classified by the multitemporal compressed Pauli features. In practice, in the SVM classification, many sub-types are defined for specific classes. For example, diverse polarimetric behaviors of the industrial and commercial areas could be observed due to their orientation, alignment and external materials. Thus, the industrial and commercial areas could be divided into several sub-classes. To achieve better classification results, those sub-classes were used in the SVM classification. After the SVM classification, those sub-classes are merged together.

4. Results and discussion

The efficiency of the multitemporal dual-orbital SAR data for urban land cover classification depends on both the efficiency of SAR data from each single date and the efficiency of their combinations. Thus, two comparisons in were made: one is comparisons of the single-date SAR classification results, which is presented in Table 2, and the other is comparison of the various multitemporal dual-orbital combinations, which are given in Table 3. From Table 2, we could see that the ascending SAR data perform slightly better than the descending ones. The major misclassification of the descending data comes from the confusion between the low-density built-up areas and the forest. The descending data, however, perform better for classification of high-density built-up areas. Therefore, complement information could be explored by combining the ascending and descending data. In terms of dates, results from A2 (5^{th} July) and A3 (22^{nd} August) have higher classification accuracy than that of the other dates. Since the incident angles are almost the same and the urban area are relatively stable in the observation time-span, the difference of the multitemporal data in the same orbital mode are mainly caused by the temporal characters of the vegetations.

Table 2. Comparison of the Classification Accuracies for Single-Date SAR Data

	A1 (Jun. 11)	A2 (Jul. 05)	A3 (Aug. 22)	A4 (Sep. 15)	D1 (Jun. 19)	D2 (Aug. 06)
OA	71.5051%	76.1293%	75.1457%	70.8880%	68.6028%	69.6603%
Kappa	0.6813	0.7316	0.7202	0.6732	0.6435	0.6555

The classification results of multitemporal SAR data are shown in Table 3. It is observed that classification of all ascending data from four-date A1234 is not as good as that of the three-date data combination from both orbits, i.e., A1+D12, A2+D12, A3+D12 and A4+D12. The descending data D12 is not as good as some two-dates combinations such as A3+D1, A2+D2. These observations confirm that the ascending and descending data provide complementary information. Further, the significance of the temporal relationships is also revealed. For example, A3+D1 and A4+D1 perform much better than A1+D1, A2+D1. This is mainly due to the fact that A3+D1 and A4 +D1 have wider time span than the other two combinations. The same phenomenon could also be observed where A1+D2 and A2+D2 are better than A3+D2 or A4+D2. These observations are further confirmed by the comparison of three-date and four-date combinations. A 123 and A12+D1 have the lowest classification accuracy than other three-date combinations. From Table 3, it is also

observed that the classification accuracy improves by adding multitemporal data. For example, A123 and A124 produce better accuracies than A12. However, this trend slows down after two descending data and one ascending data are included. Although the best result could be achieved by combining all SAR data, i.e., A1234+D12, three-date combination using data from one ascending date and two descending dates such as A2+D12, A3+D12, A4+D12 could produce similar results.

Table 3. Comparison of of the Classification Accuracies for Multitemporal SAR Data

	A1+D1	A2+D1	A3+D1	A4+D1	A1+D2	A2+D2	A3+D2
OA	0.8266	0.8054	0.8677	0.8752	0.8601	0.8774	0.8378
Kappa	0.8034	0.7813	0.8501	0.8584	0.8417	0.8612	0.8165
	A4+D2	D12	A12	A23	A123	A124	A234
OA	0.8069	0.8540	0.8054	0.8292	0.8301	0.8521	0.8655
Kappa	0.7816	0.8347	0.7805	0.8064	0.8075	0.8329	0.8475
	A1+D12	A2+D12	A3+D12	A4+D12	A12+D1	A12+D2	A12+D12
OA	0.8918	0.9058	0.9046	0.9078	0.8372	0.8845	0.9043
Kappa	0.8775	0.8934	0.8919	0.8954	0.8161	0.8692	0.8915
	A123+D1	A123+D2	A123+D12	A124+D12	A134+D12	A1234	A1234+D12
OA	0.8761	0.8944	0.9114	0.9190	0.9036	0.8617	0.9198
Kappa	0.8596	0.8802	0.8998	0.9082	0.8908	0.8433	0.9091

Table 4 presents the confusion matrices of the three-date combination A3+D12 using Compressed Logarithmic Filtered Pauli parameters. Most of the classes have greater than 90% overall accuracy. Confusion exists among high-density built-up areas, low-density areas and industry, pasture and parks as well as water and golf courses due to their similar backscatter characteristics. Fig. 2 shows the selected samples of the classification results using the three-date SAR combination.

Table 4. Confusion Matrix from Classification of the Three-Date Combination A3+D12 with Compressed Logarithmic Filtered Pauli parameters

	LD	HD	Park	Ind.	Cons.	Golf	Water	Pasture	Forest	Crop1	Crop2
LD	96.84	11.4	0.8	1.31	0.21	0	0	0	2.58	0	0
HD	3.16	81.08	0	8.79	0	0	0	0	3.05	0	0
Park	0	0.01	90.5	3.34	3.72	2.24	0.15	9.86	1.08	0.55	0.46
Ind.	0	7.51	0	86.48	0	0	0	0	0	0	0
Cons.	0	0	0.47	0	95.7	0.13	0	0.04	0	0	0.78
Golf	0	0	3.07	0	0	95.19	9.18	0.71	0	0	0
Water	0	0	0	0	0	1.9	90.67	0	0	0	0
Pasture	0	0	0.68	0	0	0	0	85.3	0.95	1	0.23
Forest	0	0	2.65	0	0	0	0	0	90.13	0.66	1.88
Crop1	0	0	1.83	0	0.26	0.53	0	3.86	2.21	96.83	0.55
Crop2	0	0	0	0.08	0.1	0	0	0.22	0	0.97	96.11
Pro.	96.84	81.08	90.5	86.48	95.7	95.19	90.67	85.3	90.13	96.83	96.11
User.	69.45	88.07	83.72	89.18	93.95	84.42	96.85	96.55	95.14	86.82	99.42

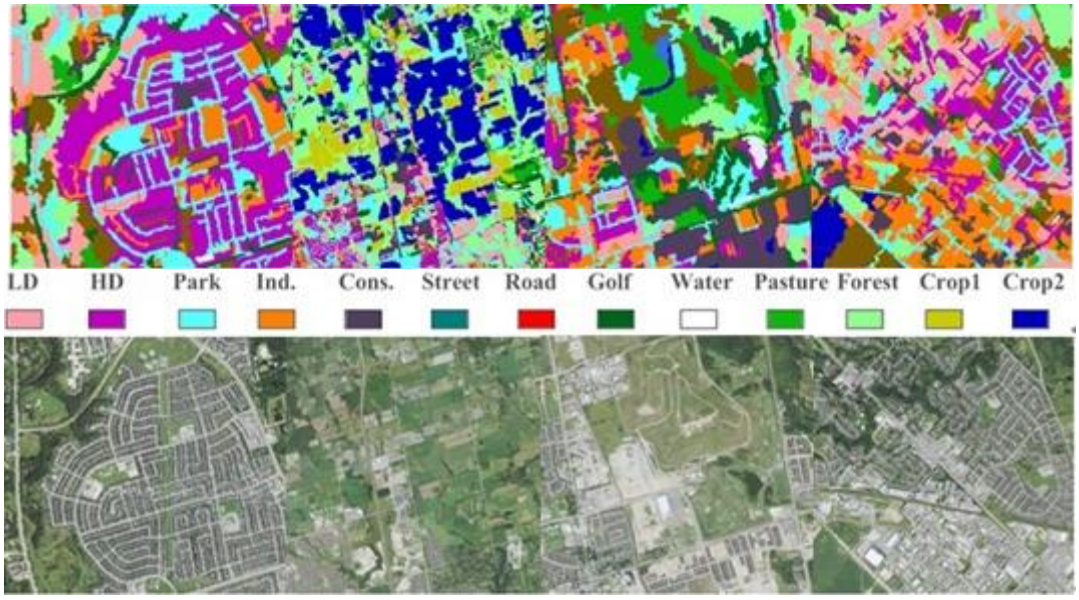

Figure 2. Selected samples of the classification results by Compressed Logarithmic Pauli parameters. Up: SVM results. Bottom: corresponding ground truths

5. Conclusion

This research investigates multitemporal dual-orbital RADARSAT-2 high-resolution polarimetric SAR data for urban land cover mapping using an object-based SVM. Using the compressed filtered Log Pauli parameters, the results show that the classification accuracy improves using by adding multitemporal data. However, this trend slows down after two descending data and one ascending data are included. The best overall classification accuracy of 92% and Kappa coefficient 0.91 is achieved using all six-date multitemporal SAR data. Similar results, however, could be achieved using three-date combination, i.e., SAR data from one ascending date and two descending dates. The results indicated that SAR data from both ascending and descending orbits provide complementary information and attention should be given to temporal relationships when plan multitemporal SAR data acquisitions.

Acknowledgements

The authors thank the Swedish National Space Board for funding this research and the Canadian Space Agency for providing the RADARSAT-2 polarimetric SAR data.

References

[1] Ainsworth, T. L., Schuler, D. L. and Lee, J.-S., 2008. *Polarimetric SAR characterization of man-made structures in urban areas using normalized circular-pol correlation coefficients*. Remote Sensing of Environment, 112, pp. 2876-2885.

[2] Alberga, V., 2007. *A study of land cover classification using polarimetric SAR parameters*. International Journal of Remote Sensing, 28, pp. 3851-3870.

[3] Alberga, V., Satalino, G. and Staykova, D. K., 2008. *Comparison of polarimetric SAR observables in terms of classification performance*. International Journal of Remote Sensing, 29, pp. 4129-4150.

[4] Chaabouni-Chouayakh, H. and Datcu, M., 2010. *Backscattering and Statistical Information Fusion for Urban Area Mapping Using TerraSAR-X Data*. IEEE Journal of Selected Topics in Applied Earth Observations and Remote Sensing, 3, pp.718-730.

[5] Esch, T., Thiel, M., Schenk, A., Roth, A., Muller, A. and Dech, S., 2010. *Delineation of Urban Footprints From TerraSAR-X Data by Analyzing Speckle Characteristics and Intensity Information*. IEEE Transaction on Geoscience and Remote Sensing, 48, pp.905-916.

[6] Niu, X. and Ban, Y., 2010. *Multitemporal RADARSAT-2 Polarimetric SAR Data for Urban Land Cover Classification using Support Vector Machine*. In 30th EARSeL Symposium, June 2010, Paris, France, pp. 581-588.

[7] Blaschke, T. 2010. *Object based image analysis for remote sensing*. ISPRS Journal of Photogrammetry and Remote Sensing, 65, pp. 2-16.

[8] Ban, Y., Hu, H. and Rangel, I. M., 2010. *Fusion of QuickBird MS and RADARSAT SAR data for urban land-cover mapping: object-based and knowledge-based approach*. International Journal of Remote Sensing, 31, pp.1391-1410.

[9] Hu, H. and Ban, Y., 2008. *Urban landuse/land-cover mapping with high-resolution SAR imagery by integrating support vector machines into object-based analysis*. In SPIE Conference on Remote Sensing for Environmental Monitoring, GIS Applications, and Geology VIII, 7110, pp. 71100K1-8.

[10] Huang, C., Davis, L. S. and Townshend, J. R. G., 2002. *An assessment of support vector machines for land cover classification*. International Journal of Remote Sensing, 23, pp. 725–749.

[11] Pal, M. and Mather, P. M., 2005. *Support vector machines for classification in remote sensing*. International Journal of Remote Sensing, 26, pp. 1007–1011.

[12] Tzotsos, A., 2006. *A support vector machine approach for object based image analysis*. In 1st International Conference on Object-based Image Analysis, Salzburg, Austria. CD-ROM.

[13] Buddhiraju, K.M. and Rizvi, I.A., 2010. *Comparison of CBF, ANN and SVM classifiers for object based classification of high resolution satellite images*. In IEEE International Conference on Geoscience and Remote Sensing Symposium, IGARSS, July 2010, Honolulu, HI, pp.40-43.

[14] Tzotsos, A. and Argialas, D. 2008. *Support Vector Machine Classification for Object-Based Image Analysis*. In Object-Based Image Analysis – Spatial Concepts for Knowledge-Driven Remote Sensing Applications, T. Blaschke, S. Lang and G. J. Hay (Eds.), pp. 663–667.

[15] Furberg, D. and Y. Ban., 2008. *Satellite Monitoring of Urban Sprawl and Assessing the Impact of Land Cover Changes in the Greater Toronto Area*. In 21th ISPRS Congress, July 2008, Beijing, China, pp. 131-136.

[16] Chang, C.-C. and Lin, C.-J., 2010. *LIBSVM: A library for support vector machines*. Available online at: http://www.csie.ntu.edu.tw/~cjlin/libsvm/ (accessed 26 January 2011).

[17] Muller, K.-R., Mika, S., Ratsch, G., Tsuda, K., and Scholkopf, B., 2001. *An introduction to kernel-based learning algorithms*. IEEE Transaction on Neural Networks, 12, pp.181-201.